2nd Quarter report (03/30/2007)

N. N. Gorelenkov, R. V. Budny, D. McCune, J. Manickam
Princeton Plasma Physics Laboratory, Princeton University

Quarterly Milestone: Analyze the normal shear discharges, performing a parameter scan to determine the linear stability of toroidal mode number n = 1-15 TAE modes.

Executive summary. The second quarter milestone was met. The stability of Alfvén Eigenmodes with frequencies up to the frequency of the TAE gap was simulated with n ranging from 1 to 20, which exceeds the planned value, n=15. Five equilibria with normal-shear safety-factor profiles were studied. The NBI injection angle was varied in order to investigate the possibility of TAE stability control. We found the expected medium to high-n range of TAEs unstable when the NBI was aimed slightly off axis. In contrast plasmas with on-axis and stronger off-axis injected beams are marginally unstable against TAEs. NBI ions have a strong contribution to the instability and thus be instrumental in TAE stability control.

The NOVA-K MHD-kinetic-hybrid code is used to study TAE stability. Using the unperturbed TAE structure calculated by the ideal MHD code, NOVA, perturbative theory in a quadratic form is applied in evaluating Alfvén mode stability. Several important kinetic damping mechanisms have been incorporated into NOVA-K over the years: trapped electron collisional damping [19], ion and electron Landau damping [3], radiative [20] and continuum [21] damping. The fast ion drive is calculated with the orbit and Larmor radius effects included [22].

Previous studies [4, 5] have shown that neutral beam ions contribute as strongly as fusion alpha particles to the TAE growth rate. Hence, the model for the beam ion distribution function is of critical importance. We outline and emphasize the distribution function model in this quarter's report, specifically we start with the improved TRANSP statistics Monte-Carlo package.

Distribution function model. If the distribution function is narrow in pitch angles, which is the case with NBI in ITER, the model to describe the distribution function of beam ions, f_b, and used in NOVA calculations [4] can be applied. It was proposed that f_b can be expanded in terms of the Legendre polynomials $P_l(\chi)$, which are the eigenfunctions of the Lorentz collisional scatering operator in the kinetic equation for f_b: $f_b = \sum_l a_l(\tau) P_l(\chi)$, $\tau = -(1/3)\ln\left[\left(1+v_*^3/v_{b0}^3\right)/\left(1+v_*^3/v^3\right)\right]$, v_{b0} is the injection velocity (at $\tau = 0$), v_* is the critical velocity at which the ion collisional drag becomes comparable with the drag on electrons. The solution at a given variable τ can be easily obtained

$$\phi(\chi) = \sum_l a_{l0} e^{-l(l+1)\tau} P_l(\chi), \tag{1}$$

where $a_{l0} = (l+1/2)\int_{-1}^{+1} P_l S(\chi-\chi_0)\, d\chi$. Practically ≥ 26 are required for good accuracy for the source term in the form $S = e^{-(\chi-\chi_0)^2/\delta\chi^2}/\delta\chi\sqrt{\pi}$, and $\delta\chi = 0.1$. Pitch angle distribution, accounting for the trapping region is obtained by substituting solution of Eq.(1) into the form

$$f_\chi = \begin{cases} \phi(\chi) - \frac{1}{2}\phi(2\chi_{s+} - \chi), & \text{counter-going ions, } \chi < -\chi_s \\ \frac{1}{2}\phi(-\chi) + \frac{1}{2}\phi(\chi), & \text{trapped ions } -\chi_s < \chi < \chi_s \\ \frac{1}{2}\phi(2\chi_{s+} + \chi), & \text{co-going ions } \chi_s < \chi \end{cases}. \tag{2}$$

This accounts for proper boundary conditions at the trapped-passing region separatrix and utilizes the image method for the image beam ion sources in order to include particle reflection from pitch angle boundaries [4]. Since this technique is not exact the resulting distribution may have discontinuities if its pitch angle width is large (or $\tau \geq 1/2$). We proposed a method which results in a good approximation to the exact solution. First, we account for the discontinuity by making the distribution continuous and renormalize it to conserve particles, which we denote f'_χ. Second, we force it to become isotropic, $f_\chi = 1/2$, at $\tau \to \infty$. Applying this procedure, the pitch angle part of the distribution function is given by

$$f_\chi = \frac{4\tau^3 + f'_\chi}{8\tau^3 + 1}, \tag{3}$$

where parameters are adjusted for better agreement with the exact solution, which we find by performing Monte-Carlo simulations. We should note however that adjusteble parameters do not depend on the plasma parameters. The

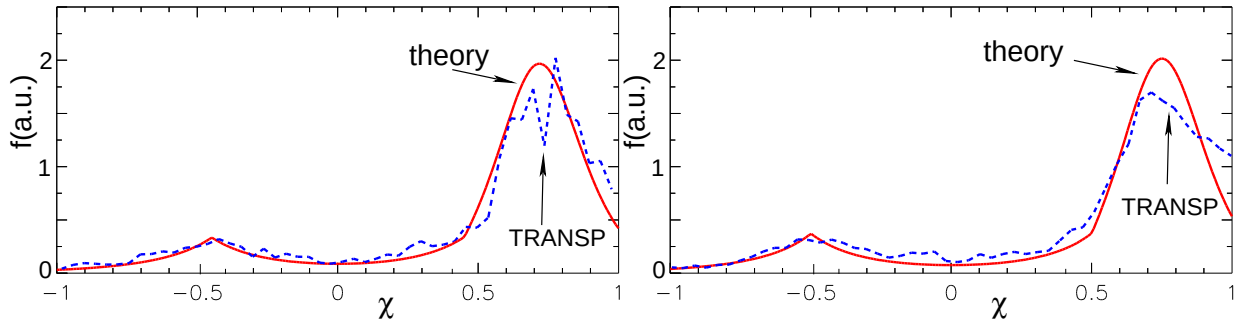

Figure 1: Results of applying the model of the beam ion pitch angle distribution function as given by Eq.(2) (theory curve) and its comparson with the TRANSP simulations (TRANSP curve) for low statistics run, $N = 10^3$ particles (left figure, distribution function is averaged over $r/a = 0.3 - 0.7$ range in minor radius) and high statistics run, $N = 10^5$ particles. In this case we used the low aspect ratio approximation for parameters $\delta\chi = 0.12$ and $r/R = 1/6$.

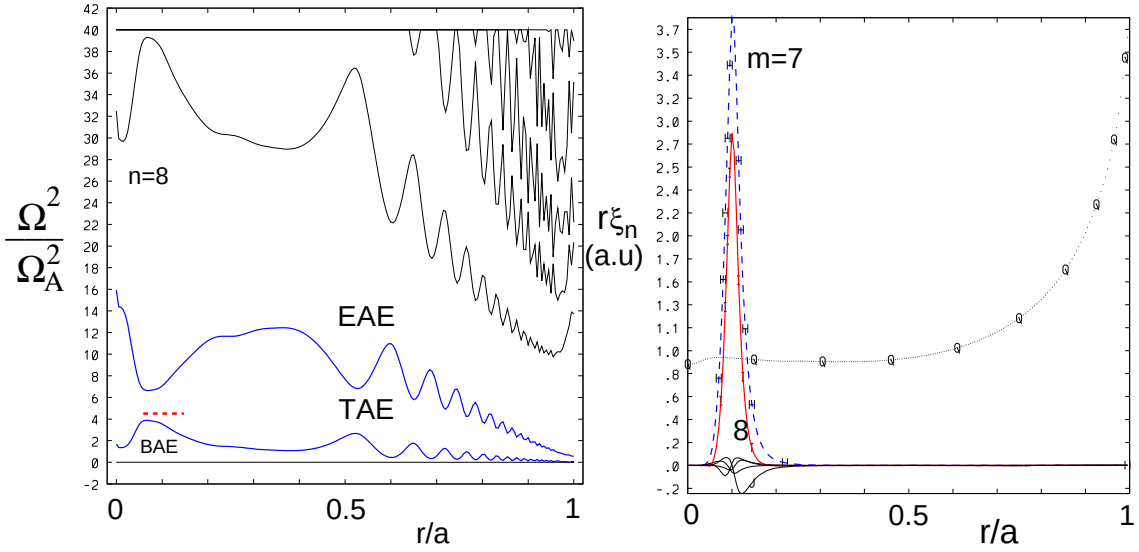

Figure 2: Ideal MHD continuum for ITER normal shear H-mode plasma run #20000T02 (left figure) and the most unstable core localized TAE poloidal harmonic radial structure for this case with NBI aiming $10cm$ below the magnetic axis. The radial extent of this mode is shown in the left figure as a dashed line corresponding to the normalized TAE eigenfrequency.

comparison with numerical simulations is shown in Fig. 1. It is notable that in both cases with low and high statistics model distribution reproduces functional pitch angle dependences of the numerical TRANSP simulated distribution. The advantage of using the model distribution is that it allows to take appropriate derivatives, which are apparently smooth.

Ideal MHD continuum. As an example we present MHD continuum for ITER plasma with slightly off-axis NBI heating, which is the most unstable studied case #20000T02 (figure 2). Another example is for the less unstable plasma with stronger off axis beam injection #20100T03 (figure 3) with NBI aiming $20cm$ below the magnetic axis. These plasmas have sawteeth, which is reflected in the low shear region inside the $r/a = 0.5$ surface. The plasma current was ramped up relatively fast in these plasma configurations, Fig.(5) of the 1st quater report. This resulted in a low shear central region, whereas in previous studies [4] the low-shear region was located near $r/a = 0.5$ giving rise to TAEs localized in that region, and determining the stability properties. As one can see from Figs. 2 and 3 localized TAE modes are present in the low shear region. Other global modes, which couple low shear and the plasma edge regions were also found but are subject to stronger damping mechanisms, such as continuum and radiative damping, which are large at high safety-factor shear, typical of the plasma edge.

TAE stability in normal shear plasmas. The list of analyzed plasmas in this case is given in the table III of the 1st quater report. We present stability simulation results with α-particles only and with alphas and beams contributing to the drive in Figs. 4, 5, and 6. Negative (positive) growth rates indicate that the modes are stable (unstable).

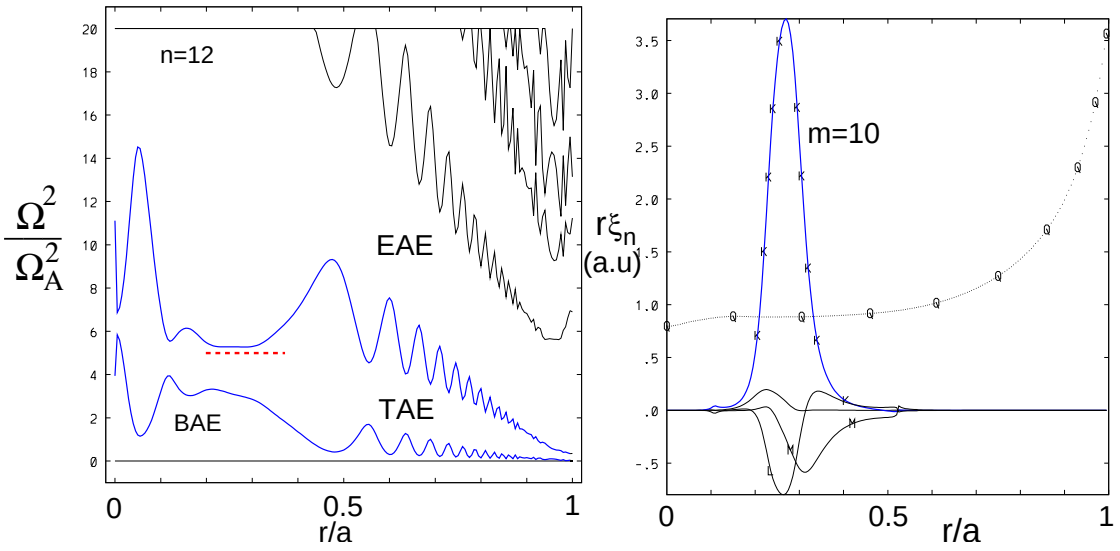

Figure 3: Ideal MHD continuum for ITER normal shear H-mode plasma run #20100T03 (left figure) and the unstable low shear localized TAE poloidal harmonic radial structure for this case with NBI aiming $20cm$ below the magnetic axis. The radial extent of this mode is shown in the left figure as a dashed line corresponding to the normalized TAE eigenfrequency.

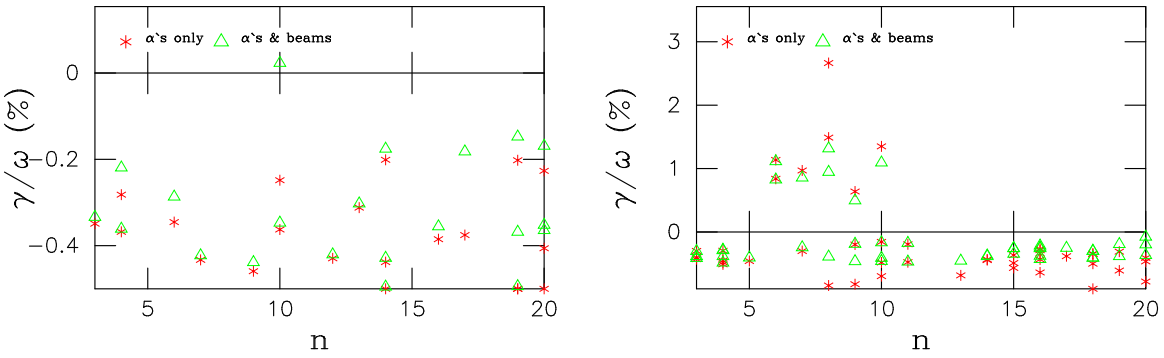

Figure 4: Toroidal mode number dependence of the AEs growth rates for the instabilities driven by alpha particles only ($*$ points), and driven by both NBI ions and alpha particles ($\triangle$ points). Results are for on-axis $Y = 0$ NBI, ITER TRANSP run #20000T01 (left figure) and for the run #20000T02 with $Y = -10cm$ (right figure).

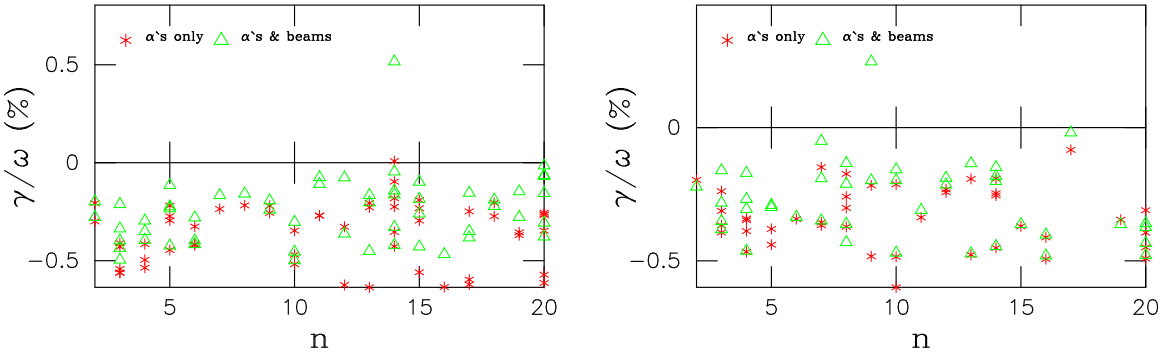

Figure 5: The same as in figure 4 but for $Y = -20$, #20100T03 run (left figure) and for the run #20100T02 with $Y = -38cm$ (right figure).

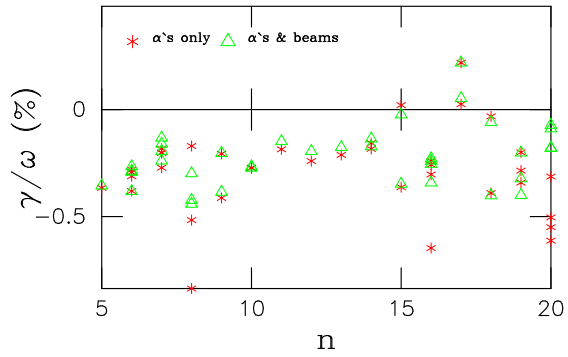

Figure 6: The same as in figure 4 but for $Y = -50$, #20000T03 run.

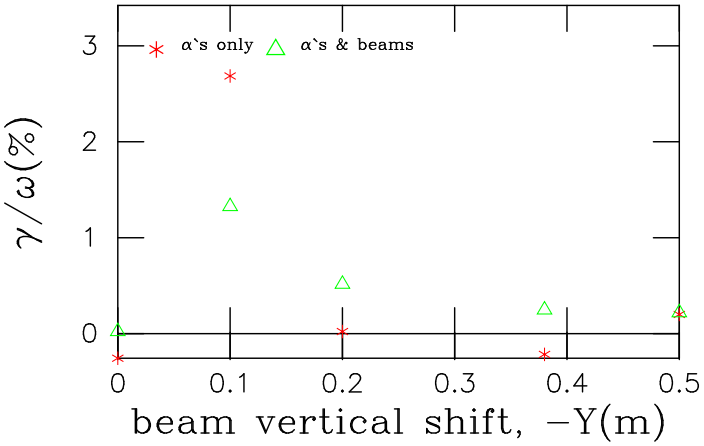

Figure 7: TAE growth rates vs. vertical deviation of the beam injection from the magnetic axis.

Summarizing the TAE stability for the normal shear H-mode plasma we plot total TAE growth rates vs. vertical deviation of the NBI aiming point from the magnetic axis, Fig, 7. On-axis beam injection seems to be stable, whereas aiming $10cm$ below the axis represents the most unstable case with the growth rates reaching 2.5% due to centrally peaked α-particle pressure profile. This is a result of the geometric optics of the NBI. Aiming below the midplane at lower values of Y shows stabilizing effects, as the beam is injected at regions with higher shear. The unstable TAEs are localized to the region of low shear within $r/a < 0.5$ in all cases of normal shear plasmas investigated.

It seems likely that such localized TAEs will not result in any significant effects on fast ion confinement, but may transport them radially toward the edge where TAE avalanches could be formed.

[1] C. Z. Cheng and M. S. Chance, Phys. Fluids **29**, 3695 (1986).
[2] G. Y. Fu and J. W. V. Dam, Phys. Fluids B **1**, 1949 (1989).
[3] C. Z. Cheng, Phys. Reports **211**, 1 (1992).
[4] N. N. Gorelenkov, H. L. Berk, and R. V. Budny, Nucl. Fusion **45**, 226 (2005).
[5] N. N. Gorelenkov, H. L. Berk, R. V. Budny, C. Z. Cheng, G. Y. Fu, W. W. Heidbrink, G. J. Kramer, D. Meade, and R. Nazikian, Nucl. Fusion **43**, 594 (2003).
[6] D. J. Campbell, Phys. Plasmas **8**, 2041 (2001).
[7] D. Campbell, F. D. Marco, G. Giruzzi, G. Hoang, L. D. Horton, G. Janeschitz, J. Johner, and et. al., in *Proceedings of 21th IAEA Fusion Energy Conference*, Chengdu, China) **IAEA-CN-149-FT/1-1**, 1 (2006).
[8] O. Gruber, J. Hobirk, C. F. Maggi, and et al., Plasma Phys. Contr. Fusion **47**, B135 (2005).
[9] E. Joffrin, A. C. C. Sips, J. F. Artaud, and et. al., Nucl. Fusion **45**, 626 (2005).

[10] M. R. Wade, T. C. Luce, P. A. Politzer, and et al., Phys. Plasmas **8**, 2208 (2001).
[11] R. E. Waltz, G. M. Staebler, W. Dorland, and et al., Phys. Plasmas **4**, 2482 (1997).
[12] P. Strand, H. Nordman, J. Weiland, and J. P. Christiansen, Nucl. Fusion **38**, 545 (1998).
[13] S. C. Jardin, N. Pomphrey, and J. J. Delucia, J. Comput. Phys. **46**, 481 (1986).
[14] R. V. Budny, Nucl. Fusion **42**, 1383 (2002).
[15] A. Pankin, D. McCune, R. Andre, and et.al., Comp. Phys. Communications **159**, 157 (2004).
[16] M. Brambilla, Plasma Phys. Contr. Fusion **41**, 1 (1999).
[17] M. Evrard, J. Ongena, and D. van Eester, in *AIP Conference Proceedings 335, Radio-Frequency Power in Plasmas, 11th topical conference*, Palm Springs **335**, 235 (1995).
[18] R. V. Budny and C. E. Kessel, to be submitted (2007).
[19] G. Y. Fu, C. Z. Cheng, and K. L. Wong, Phys. Fluids B **5**, 4040 (1993).
[20] G. Y. Fu, C. Z. Cheng, R. Budny, Z. Chang, D. S. Darrow, E. Fredrickson, E. Mazzucato, R. Nazikian, K. L. Wong, and S. Zweben, Phys. Plasmas **3**, 4036 (1996).
[21] N. N. Gorelenkov, Phys. Rev. Letters **95**, 265003 (2005).
[22] N. N. Gorelenkov, C. Z. Cheng, and G. Y. Fu, Phys. Plasmas **6**, 2802 (1999).